THE JOURNAL OF BIOLOGICAL CHEMISTRY VOL. 286, NO. 15, pp. 13052–13059, April 15, 2011

Orderly Inactivation of the Key Checkpoint Protein Mitotic Arrest Deficient 2 (MAD2) during Mitotic Progression*[S]

Received for publication, November 9, 2010, and in revised form, February 17, 2011 Published, JBC Papers in Press, February 18, 2011, DOI 10.1074/jbc.M110.201897

Hoi Tang Ma and Randy Y. C. Poon[1]

From the Division of Life Science, Hong Kong University of Science and Technology, Clear Water Bay, Hong Kong, China

Anaphase is promoted by the ubiquitin ligase anaphase-promoting complex/cyclosome (APC/C) only when all the chromosomes have achieved bipolar attachment to the mitotic spindles. Unattached kinetochores or the absence of tension between the paired kinetochores activates a surveillance mechanism termed the spindle-assembly checkpoint. A fundamental principle of the checkpoint is the activation of mitotic arrest deficient 2 (MAD2). MAD2 then forms a diffusible complex called mitotic checkpoint complex (designated as $MAD2^{(MCC)}$) before it is recruited to APC/C (designated as $MAD2^{(APC/C)}$). Large gaps in our knowledge remain on how MAD2 is inactivated after the checkpoint is satisfied. In this study, we have investigated the regulation of MAD2-containing complexes during mitotic progression. Using selective immunoprecipitation of checkpoint components and gel filtration chromatography, we found that $MAD2^{(MCC)}$ and $MAD2^{(APC/C)}$ were regulated very differently during mitotic exit. Temporally, $MAD2^{(MCC)}$ was broken down ahead of $MAD2^{(APC/C)}$. The inactivation of the two complexes also displayed different requirements of proteolysis; although APC/C and proteasome activities were dispensable for $MAD2^{(MCC)}$ inactivation, they are required for $MAD2^{(APC/C)}$ inactivation. In fact, the degradation of CDC20 is inextricably linked to the breakdown of $MAD2^{(APC/C)}$. These data extended our understanding of the checkpoint complexes during checkpoint silencing.

Activation and inactivation of cyclin-dependent kinase 1 (CDK1) are key events that control entry and exit of mitosis, respectively. CDK1 activation is mediated by cyclin B binding and T-loop phosphorylation. On the other hand, CDK1 inactivation is triggered by the destruction of cyclin B, which is carried out by the ubiquitin ligase APC/C[2] in association with a targeting subunit called CDC20 (1).

Activation of APC/C is initiated only when all the chromosomes have achieved bipolar attachment to the mitotic spindles. Unattached kinetochores or the absence of tension between the paired kinetochores activate a surveillance mechanism termed the spindle-assembly checkpoint (2). In essence, unattached kinetochores attract components of the checkpoint machinery, which then catalyzes the formation of a diffusible complex called the MCC (mitotic checkpoint complex); components include MAD2, BUBR1, BUB3, and CDC20. This leads to the inhibition of APC/C by MAD2 (3). According to this model, at least three populations of MAD2 are present during mitosis, including free MAD2, those serving as components of MCC, and those that bind to APC/C (4–6).

Binding to CDC20 requires a conformational change in MAD2 from a less stable open conformation (O-MAD2) to a closed conformation (C-MAD2) (7). According to a currently favored MAD2 template model, the C-MAD2 that bound to MAD1 at the kinetochores serves as a template for the conversion of the cytosolic pool of O-MAD2 into C-MAD2. The newly activated C-MAD2 then leaves the kinetochore to inhibit CDC20 (8). The MAD2-CDC20 complexes also autoamplify the checkpoint signal by converting more O-MAD2 into C-MAD2 (7).

After all kinetochores are properly attached, the checkpoint is terminated to allow sister chromatid separation. The essential question regarding exactly how the checkpoint is silenced remains incompletely understood. A number of mechanisms have been proposed. These include the stripping of checkpoint components from the kinetochore by a dynein motility-dependent mechanism, the dissociation of MAD2-CDC20 by APC/C-dependent mechanisms, and the neutralization of MAD2 by a MAD2-binding protein called $p31^{comet}$ (2). More recently, PP1 is also implicated in reversing the phosphorylation critical for maintaining the checkpoint (9, 10).

Although progress in the past several years has unraveled some underlying principles on checkpoint silencing, large gaps in our knowledge remain. In this study, we have investigated the temporal regulation of MAD2-containing complexes during mitotic progression in human cells. Our data revealed that $MAD2^{(MCC)}$ and $MAD2^{(APC/C)}$ were regulated very differently during mitotic exit. Temporally, $MAD2^{(MCC)}$ was broken down ahead of $MAD2^{(APC/C)}$. In addition, the inactivation of the two complexes also displayed different requirements of proteolysis.

EXPERIMENTAL PROCEDURES

Materials—All reagents were obtained from Sigma-Aldrich unless stated otherwise.

DNA Constructs and siRNAs—The NcoI-NcoI fragment from FLAG-3C-cyclin B1(CΔ62)-EGFP in pUHD-P3 (11) was ligated into mRFP1 in pUHD-P3T (11). A puromycin-resistant cassette was inserted into the BamHI site to create mRFP1-cyclin B1(CΔ62) in pUHD-P3T (to use as the APC/C reporter). FLAG-cyclin B1(NΔ88) in pUHD-P1 was constructed as

* This work was supported in part by the Research Grants Council Grants 662007 and 662208 (to R. Y. C. P.).

[S] The on-line version of this article (available at http://www.jbc.org) contains supplemental Figs. S1–S4.

[1] To whom correspondence should be addressed. Tel.: 852-23588703; E-mail: rycpoon@ust.hk.

[2] The abbreviations used are: APC/C, anaphase-promoting complex/cyclosome; MCC, mitotic checkpoint complex; MAD2, mitotic arrest deficient 2; mRFP, monomeric red fluorescent protein.

described previously (12). A puromycin-resistant gene cassette was inserted into the BamHI site. Stealth siRNAs targeting human APC2 (443–467), CDC20 (963–986), cyclin B1 (937–961), CDC27 (2037–2061), and control siRNA were obtained from Invitrogen (numbers represent the position of the targeting sequence in the ORF). CDC16 siRNA (525–543) was obtained from RiboBio (Guangzhou, China).

Cell Culture—The HeLa cell line used in this study is a clone that expressed the Tet-Off tetracycline repressor chimera (13). To generate stable APC/C reporter cells, HeLa cells stably expressing histone H2B-GFP (12) were transfected with mRFP1-cyclin B1(CΔ62) in pUHD-P3T and selected with puromycin. To generate inducible cyclin B1(NΔ88)-expressing cells, HeLa cells were transfected with FLAG-cyclin B1(NΔ88) in pUHD-P1 and selected with puromycin in the presence of doxycycline. Mixed population was isolated after about 2 weeks of selection. Cells were treated with the following reagents at the indicated final concentration: doxycycline (2 μg/ml), MG132 (10 μM), nocodazole (0.33 μM), and RO3306 (Enzo Life Sciences) (10 μM). Preparation of cell-free extracts was performed as described (14). Cells were transfected with plasmids or siRNA using a calcium phosphate method (15) or Lipofectamine™ RNAiMAX (Invitrogen), respectively.

Cell Cycle Synchronization—Double thymidine synchronization was performed as described (13). Details on synchronization are described in supplemental Fig. S1. Transfection of siRNA was performed after the release from the first thymidine block.

Antibodies and Immunological Methods—Immunoblotting and immunoprecipitation were performed as described previously (14). Monoclonal antibodies against cyclin A2 (16) and cyclin B1 (12) and polyclonal antibodies against CDK1 (17) were obtained from the same sources described in those references. Polyclonal antibodies against and APC4 (ab72149, Abcam, Cambridge, UK), BUBR1 (A300-386A), CDC16 (A301-165A-1) (Bethyl Laboratories, Montgomery, TX), CDC20 (sc-8358), phospho-histone $H3^{Ser10}$ (sc-8656R), and securin (sc-56207) (Santa Cruz Biotechnology, Santa Cruz, CA) and monoclonal antibodies against CDC20 (sc-5296, Santa Cruz Biotechnology), MAD2, and CDC27 (BD Transduction Laboratories) were obtained from the indicated suppliers. Polyclonal antiserum against MAD2 was raised against bacterially expressed GST-MAD2.

Gel Filtration Chromatography—Lysates (2 mg in 100 μl) were applied onto a Superose 6 GL column (GE Healthcare, Little Chalfont, UK), and chromatography was conducted using an ÄKTA™ FPLC system (GE Healthcare) using the buffer 50 mM Tris-HCl, pH 7.5, 100 mM NaCl, 50 mM NaF, 1 mM EDTA, and 1 mM DTT with a flow rate of 0.5 ml/min. Fractions (250 μl) were collected and mixed with 50 μl of SDS sample buffer; 15 μl was then analyzed by immunoblotting.

Time-lapse Microscopy—Time-lapse microscopy was performed exactly as described previously (11).

RESULTS

Evidence That $MAD2^{(MCC)}$ and $MAD2^{(APC/C)}$ Are Differentially Regulated during Mitosis—At least three populations of MAD2 are present during mitosis: free MAD2, those serving as components of MCC (designated herein as $MAD2^{(MCC)}$), and those that bind to APC/C (designated herein as $MAD2^{(APC/C)}$) (see also Fig. 6*B*). To study these complexes during various stages of mitosis, HeLa cells were synchronized by a series of traps and releases. A summary of the synchronization procedures is shown in supplemental Fig. S1. All procedures began with a basic double thymidine block protocol. Releasing cells from the block (8 h) yielded G_2 cells. Prometaphase cells were enriched by trapping cells with nocodazole followed by shake off. Lastly, metaphase cells were obtained by releasing cells from the nocodazole block in the presence of the proteasome inhibitor MG132. The loss of MAD2 staining from kinetochores validated that the cells were trapped in a metaphase-like state (supplemental Fig. S2).

The presence of $MAD2^{(APC/C)}$ and $MAD2^{(MCC)}$ was initially examined by co-immunoprecipitation (Fig. 1*A*). As expected, MAD2 was present in CDC20 immunoprecipitates from prometaphase lysates (*lane 6*) (18). In contrast, MAD2 was absent in the immunoprecipitates from G_2 lysates (*lane 5*) despite similar concentrations of total MAD2 in the two lysates (*lanes 1* and *2*). Likewise, CDC20 was present in the reciprocal immunoprecipitation using an antiserum against MAD2 from prometaphase but not G_2 lysates (*lanes 9* and *10*). These results verify that the spindle-assembly checkpoint was activated during prometaphase.

To specifically detect $MAD2^{(APC/C)}$ complexes, two APC/C core subunits (APC4 and CDC27) were immunoprecipitated. Fig. 1*B* shows that MAD2 associated with APC/C during prometaphase (19). The specificity of the interaction was demonstrated by the disruption of the binding after CDC20 was depleted with siRNA (Fig. 1*C*, *lane 7*). As a control, this interaction was not affected after cyclin B1 depletion (*lane 6*). Although cyclin B1 could be down-regulated without affecting entry into mitosis (20), the phosphorylation shifts of CDC27 were largely attenuated, suggesting that CDC27 phosphorylation was not required for APC/C-MAD2 interaction. Collectively, these data indicate that MAD2 interacted with APC/C during prometaphase in a CDC20-dependent manner.

It has been reported that MAD2 dissociates from CDC20 during mitotic progression (18). We generated checkpoint-satisfied mitotic cells by treating nocodazole-released cells with MG132 to inhibit proteolysis. These cells formed a metaphase plate but were unable to degrade an APC/C reporter (containing mRFP1 fused to the D-box region of cyclin B1) (supplemental Fig. S1, see also later in Fig. 4*C*). Reciprocal immunoprecipitation validated that MAD2-CDC20 dissociated during metaphase (Fig. 1*A*, *lanes 8* and *12*). Unexpectedly, MAD2 still remained bound to the APC/C (CDC27 and APC4 immunoprecipitates) in metaphase lysates (Fig. 1*B*, *lanes 8* and *12*). As metaphase cells were prepared with MG132 treatment, we also incubated prometaphase cells with MG132 for the same amount of time for a more direct comparison (*lanes 7* and *11*). These experiments confirmed that although MAD2-CDC20 binding was detected only in prometaphase, $MAD2^{(APC/C)}$ was detected in both prometaphase and metaphase.

Given that CDC20 is an integral component of both $MAD2^{(APC/C)}$ and $MAD2^{(MCC)}$, it is paradoxical that only $MAD2^{(APC/C)}$ was detected during metaphase by co-immuno-

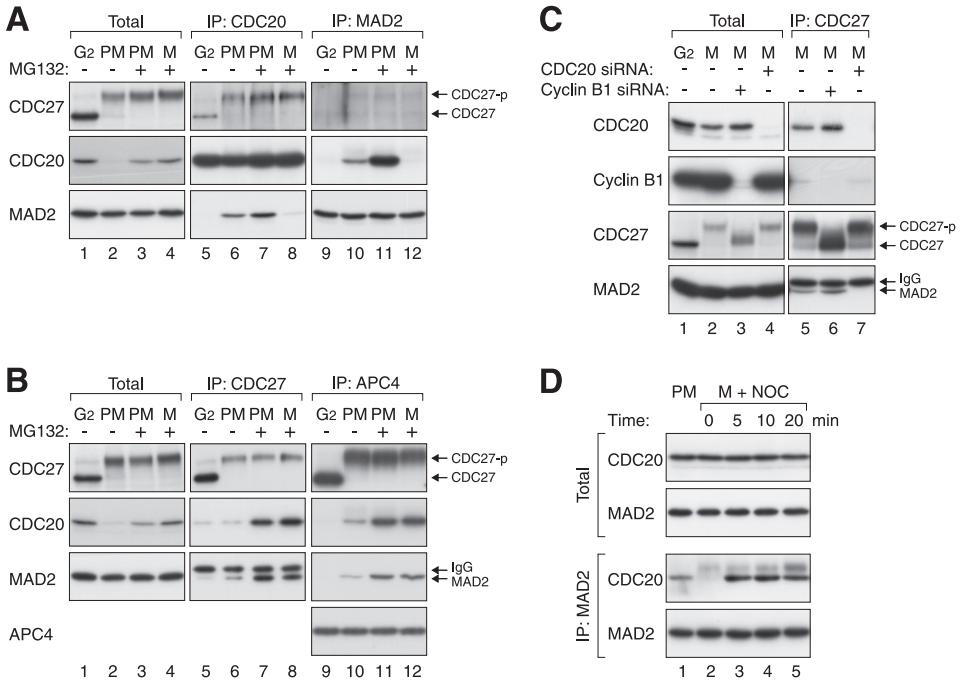

FIGURE 1. **MAD2 interacts with MCC and APC/C differentially during mitotic progression.** *A*, MAD2$^{(MCC)}$ is present in prometaphase and disappeared in metaphase. HeLa cells were synchronized in G_2, prometaphase (*PM*), or metaphase (*M*) in either the absence or the presence of MG132 (supplemental Fig. S1). Cell-free extracts were prepared and subjected to immunoprecipitation with antibodies against CDC20 and MAD2. The presence of CDC27, CDC20, and MAD2 in the total lysates and immunoprecipitates (*IP*) was detected by immunoblotting. The positions of phosphorylated (*CDC27-p*) and unphosphorylated CDC27 are indicated. *B*, MAD2$^{(APC/C)}$ is present in both prometaphase and metaphase. Cells in different cell cycle phases were prepared as in *panel A*. Lysates were prepared and subjected to immunoprecipitation with antibodies against CDC27 and APC4. Total lysates and immunoprecipitates were analyzed with immunoblotting for the indicated proteins. The upper bands in the MAD2 blot are signals from the IgG light chains. *C*, binding of MAD2 to APC/C during metaphase is CDC20-dependent. Cells were synchronized (supplemental Fig. S1) and transfected with control or siRNAs against CDC20 or cyclin B1. Lysates were prepared and subjected to immunoprecipitation with antibodies against CDC27. Total lysates and immunoprecipitates were then analyzed with immunoblotting. *D*, reappearance of MAD2$^{(MCC)}$ after reactivation of the spindle-assembly checkpoint. Prometaphase and metaphase cells were prepared as in *panel A*. Metaphase cells were then treated with nocodazole (*NOC*) and harvested at the indicated time points. Lysates were prepared and subjected to immunoprecipitation with an antiserum against MAD2. Total lysates and the immunoprecipitates were analyzed with immunoblotting.

precipitation. To resolve this dilemma, we analyzed the MAD2 complexes by gel filtration chromatography, thereby excluding possible artifacts from immunoprecipitation. Previous studies indicate that free MAD2 (<100 kDa), MCC (~670 kDa), and APC/C (>1.5 MDa) can be resolved by gel filtration chromatography (4). Fig. 2*A* shows that in G_2 lysates, MAD2 was exclusively eluted in fractions representing monomer and/or dimer of free MAD2 (21). In contrast, marginal but detectable levels of MAD2 co-eluted with APC/C components (including CDC20, APC4, and CDC27) as well as with MCC in prometaphase lysates (Fig. 2*B*). More MAD2 was found in both fractions after proteins were stabilized with MG132 (Fig. 2*C*). Both fractions disappeared after CDC20 was depleted with siRNA (supplemental Fig. S3), confirming the CDC20 dependence of MAD2$^{(MCC)}$ and MAD2$^{(APC/C)}$. Significantly, metaphase lysates contained free MAD2 and MAD2$^{(APC/C)}$ but not MAD2$^{(MCC)}$ (Fig. 2*D*).

Taken together, these results indicated that although prometaphase contained both MAD2$^{(APC/C)}$ and MAD2$^{(MCC)}$, metaphase only contained MAD2$^{(APC/C)}$. Our data also indicated that antibodies against MAD2 selectively immunoprecipitated MAD2$^{(MCC)}$ but not MAD2$^{(APC/C)}$. It is possible that MAD2 became inaccessible when bound to the large APC/C complex. In further support of this, although the majority of total MAD2 could be immunodepleted with the MAD2 antiserum, the MAD2 that bound to APC4 was not depleted (supplemental Fig. S4). By contrast, antibodies against CDC27 and APC4 were able to immunoprecipitate MAD2$^{(APC/C)}$. Nonetheless, the selective recognition of MAD2$^{(APC/C)}$ and MAD2$^{(MCC)}$ by the antibodies provided a simple method to analyze the two complexes.

Disappearance of MAD2$^{(MCC)}$ during Metaphase Is Reversible on Reactivation of the Checkpoint—Given that the disappearance of MAD2$^{(MCC)}$ appears to be correlated with checkpoint satisfaction, a prediction is that MAD2$^{(MCC)}$ should form again if the checkpoint is reactivated. For this purpose, metaphase cells were first prepared as above, before nocodazole was reintroduced to disrupt the spindles. Fig. 1*D* shows that as expected, MAD2$^{(MCC)}$ was detected in prometaphase but disappeared in metaphase. MAD2$^{(MCC)}$ was again detected immediately after nocodazole was reintroduced. These results indicate that formation of MAD2$^{(MCC)}$ was dynamically controlled by the spindle-assembly checkpoint.

MAD2$^{(APC/C)}$ but Not MAD2$^{(MCC)}$ Persists during the Anaphase-like State Induced by Non-degradable Cyclin B1—To ensure that the observed regulation of APC/C and MCC in checkpoint-satisfied samples was not simply due to a perturbation of ubiquitin equilibrium by MG132 (22), an alternative method was also used to obtain checkpoint-satisfied cells without the use of proteasome inhibitors. A non-degradable cyclin B1 lacking the N-terminal destruction box was used to trap cells in a mitotic state. A cell line that expressed cyclin B1(NΔ) under

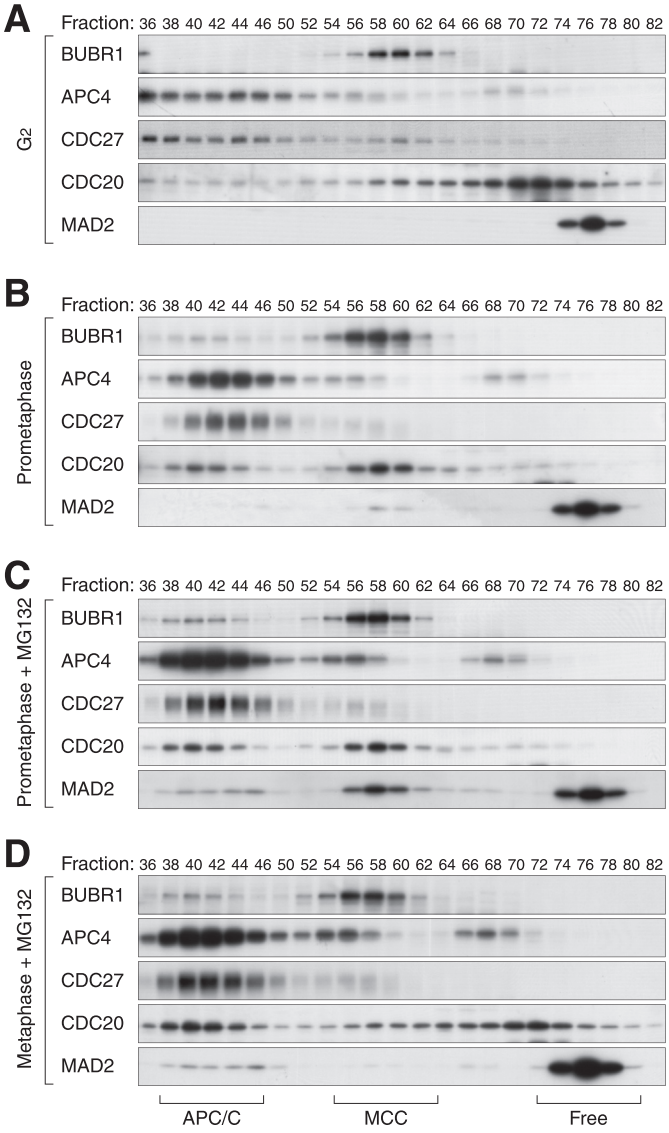

FIGURE 2. **Gel filtration analysis of MAD2-containing complexes.** Cell-free extracts were prepared from cells in G_2 phase (*A*), prometaphase (*B*), prometaphase (with MG132) (*C*), and metaphase (with MG132) (*D*) as described in supplemental Fig. S1. The extracts were applied onto gel filtration chromatography. Fractions were collected and analyzed with immunoblotting for the indicated proteins. The positions of APC/C, MCC, and free MAD2 are indicated.

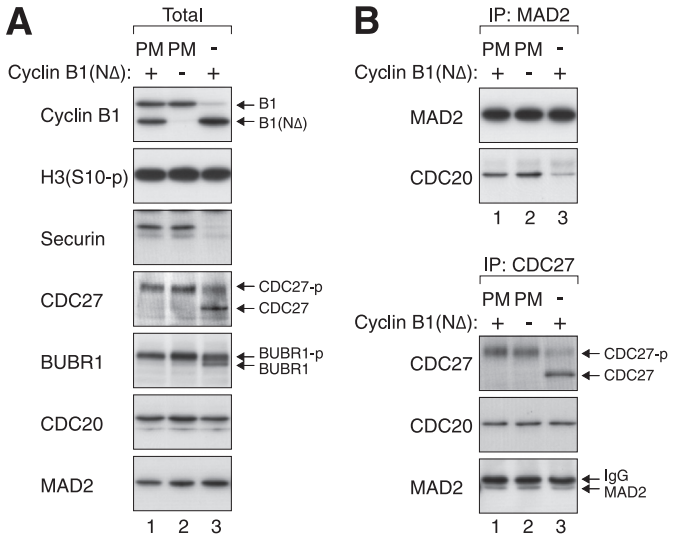

FIGURE 3. **MAD2$^{(APC/C)}$ but not MAD2$^{(MCC)}$ is present in the anaphase-like state induced by non-degradable cyclin B1.** *A*, ectopic expression of cyclin B1(NΔ) traps cells in a mitotic state with an inactive checkpoint. Inducible cyclin B1(NΔ)-expressing cells were synchronized as described in supplemental Fig. S1. Cell-free extracts were prepared and analyzed with immunoblotting. *PM*, prometaphase; *CDC27-p*, phosphorylated CDC27. *B*, MAD2$^{(MCC)}$ is absent in cyclin B1(NΔ)-blocked extracts. Cells lysates were prepared as in *panel A* and immunoprecipitated with antibodies against MAD2 (*upper panel*) or CDC27 (*lower panel*). The immunoprecipitates (*IP*) were subjected to immunoblotting to detect the indicated proteins. The upper bands in the MAD2 blot are signals from the IgG light chains.

the control of tetracycline-inducible promoter was generated. The induction of cyclin B1(NΔ) was then coupled to the synchronization procedure to minimize the toxicity due to long term expression (supplemental Fig. S1).

Non-degradable cyclin B1 can trap cells in an anaphase-like state with a satisfied checkpoint (23). Our data confirmed that cells expressing cyclin B1(NΔ) contained low amounts of APC/C substrates such as securin and cyclin B1 (Fig. 3*A*, *lane 3*). The dephosphorylation of BUBR1 also suggested that the spindle-assembly checkpoint was turned off. For a comparison, APC/C was not activated when cyclin B1(NΔ) was induced in prometaphase (*lane 1*). It is noteworthy that CDC20 remained stable when other APC/C substrates were degraded. As CDC20 is proposed to be degraded by autoubiquitination (24) as well as by CDH1 (25), it is possible that CDH1 is suppressed by the cyclin B1(NΔ)-CDK1 (26).

We next analyzed the status of MAD2$^{(MCC)}$ by immunoprecipitation. Fig. 3*B* shows that significantly less MAD2$^{(MCC)}$ was present in cyclin B1(NΔ)-blocked cells than during prometaphase. In contrast, the abundance of MAD2$^{(APC/C)}$ was unchanged between prometaphase and cyclin B1(NΔ)-blocked cells. Collectively, these data indicate that MAD2$^{(MCC)}$ was unstable during the anaphase-like state induced by cyclin B1(NΔ), further substantiating the idea that MAD2$^{(APC/C)}$ persists at the time when MAD2$^{(MCC)}$ is already removed.

MAD2$^{(MCC)}$ Disappears before MAD2$^{(APC/C)}$ during Mitotic Exit—To further verify the differential regulation of MAD2-containing complexes, we next examined their dissociation kinetics during mitotic exit. Cells were first trapped with nocodazole before being released by extensive washing. Flow cytometry analysis revealed that most cells entered G_1 at 90 min (Fig. 4*A*). To determine the time of mitotic exit more precisely, individual cells were tracked with time-lapse microscopy. For this purpose, cells expressing GFP-tagged histone H2B and an mRFP-tagged APC/C reporter (27) were used. Fig. 4*B* shows that more than half of the cells had undergone anaphase at 60 min (a representative example is shown in Fig. 4*C*). As expected, the APC/C reporter was degraded at the time of anaphase onset. By contrast, cells released from nocodazole block in the presence of MG132 were trapped in metaphase without degradation of the APC/C reporter (Fig. 4*C*).

To determine the kinetics of the breakdown of MAD2$^{(MCC)}$ and MAD2$^{(APC/C)}$ during mitotic exit, MAD2 and CDC27 were immunoprecipitated from lysates prepared at different time points after nocodazole release (Fig. 4*D*). Immunoblotting of the total lysates indicated that although cyclin B1 was destroyed abruptly at 90 min, the degradation of CDC20 started earlier

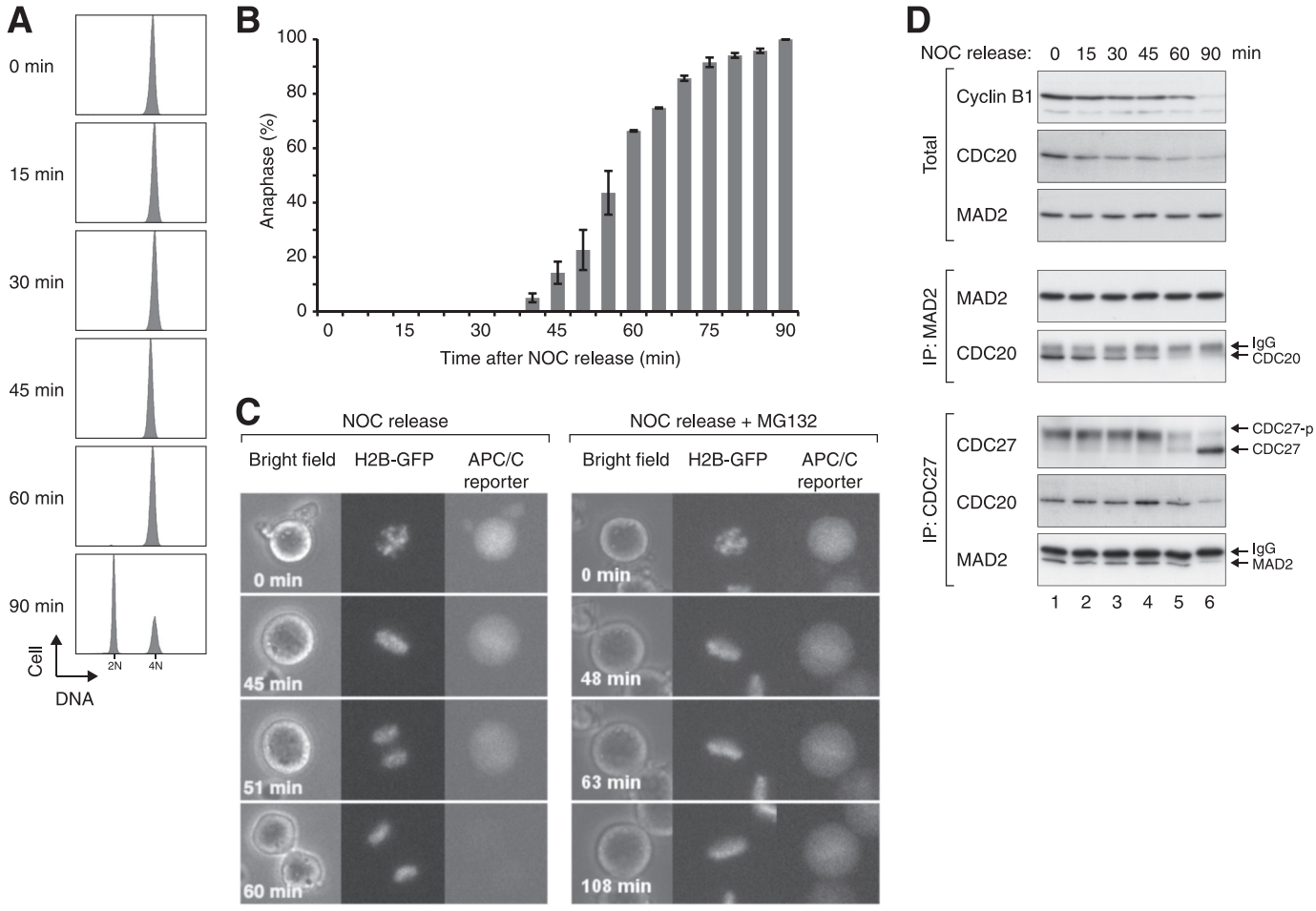

FIGURE 4. **MAD2$^{(MCC)}$ and MAD2$^{(APC/C)}$ disappear at different times during mitotic exit.** *A*, release of cells from mitosis. HeLa cells were synchronized at prometaphase with double thymidine block and nocodazole as described under "Experimental Procedures." The cells were then released into drug-free medium and harvested at the indicated time points. The DNA contents of the cells were analyzed with flow cytometry. The positions of 2N and 4N DNA contents are indicated (*N*, haploid number). *B*, anaphase occurs at ~60 min after release from the nocodazole (*NOC*) block. HeLa cells expressing both histone H2B-GFP and APC/C reporter were synchronized at prometaphase ("Experimental Procedures"). Individual cells were tracked using time-lapse microscopy. The accumulative percentage of cells undergoing anaphase was quantified ($n = 60$, mean + S.D. from two independent experiments). *C*, examples of time-lapse microscopy of mitotic exit. Cells were synchronized at prometaphase, released, and tracked with time-lapse microscopy as in *panel B*. Time-lapse images of a representative cell are shown (*left-hand panel*). Similar time-lapse microscopy of cells released from nocodazole block in the presence of MG132 is shown for comparison (*right-hand panel*). *D*, disappearance of MAD2$^{(MCC)}$ occurs before MAD2$^{(APC/C)}$ during mitotic exit. Cells were synchronized as in *panel A* and harvested at the indicated time points. Lysates were prepared and immunoprecipitated with antiserum against either MAD2 or CDC27. Total cell lysates or the immunoprecipitates (*IP*) were then analyzed with immunoblotting. *CDC27-p*, phosphorylated CDC27.

and was more progressive. The CDC20 present in the MAD2 immunoprecipitates started to decrease from 30 min and was absent by 60 min. In contrast, a significant amount of MAD2 and CDC20 was still present in the CDC27 immunoprecipitates at up to 90 min. These results indicate that MAD2$^{(MCC)}$ dissociates before MAD2$^{(APC/C)}$ during mitotic exit.

Rapid Inactivation of MAD2$^{(MCC)}$ before MAD2$^{(APC/C)}$ after Short-circuiting of the Spindle-Assembly Checkpoint—The above data demonstrated that MAD2$^{(MCC)}$ and MAD2$^{(APC/C)}$ were broken down with different kinetics when cells were released from nocodazole block. However, using this method, cells exited mitosis heterogeneously over a window of ~30 min (Fig. 4*B*). To obtain further evidence of the different dissociation kinetics of the MAD2 complexes, mitotic exit was triggered more sharply by using a CDK1 inhibitor (28). Both histone H3^{Ser10} and CDC27 were completely dephosphorylated and cyclin B1 was destroyed as quickly as 30 min after treatment with the CDK1 inhibitor RO3306 (29) (Fig. 5*A*).

The presence of MAD2$^{(MCC)}$ and MAD2$^{(APC/C)}$ after RO3306 treatment was analyzed with immunoprecipitation. Fig. 5*B* shows that MAD2$^{(MCC)}$ was rapidly eliminated after RO3306 treatment (*lanes 1–3*). MAD2$^{(APC/C)}$ was likewise removed, albeit with slower kinetics (Fig. 5*C*). A caveat of these results is that they may be caused by the significant reduction of total CDC20 after RO3306 treatment (Fig. 5*A*). To exclude the contribution of CDC20 degradation, mitotic cells were incubated with MG132 before the RO3306 challenge. As expected, MG132 stabilized both cyclin B1 and CDC20 but did not interfere with mitotic exit (dephosphorylation of histone H3^{Ser10} and CDC27) (Fig. 5*A*, *lanes 4–6*). The slight delay in histone H3^{Ser10} dephosphorylation may be due to the delay in activation of proteasome-dependent phosphatases (30). Even after CDC20 was stabilized by MG132, MAD2$^{(MCC)}$ was still eliminated rapidly after RO3306 treatment (Fig. 5*B*). In contrast, CDC20 and MAD2 remained bound to CDC27 under the same conditions (Fig. 5*C*), indicating that MAD2$^{(APC/C)}$ was more stable than MAD2$^{(MCC)}$.

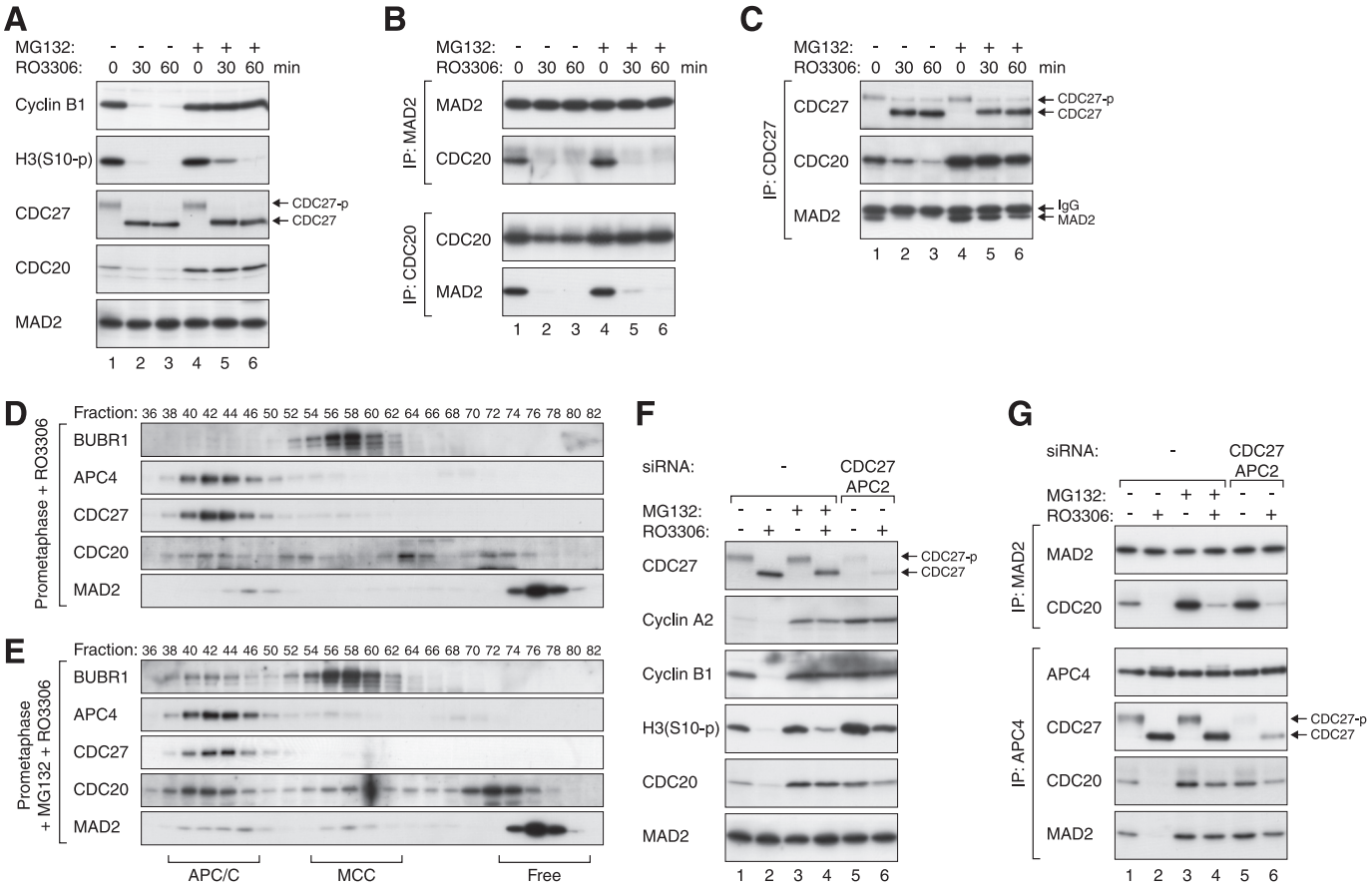

FIGURE 5. **Selective dissociation of MAD2$^{(MCC)}$ after RO3306-induced mitotic exit.** *A*, RO3306 induces rapid mitotic exit. HeLa cells were enriched in prometaphase as described in supplemental Fig. S1. The cells were pretreated with either dimethyl sulfoxide (DMSO) or MG132 for 1 h before being incubated with RO3306. The cells were harvested at the indicated time points. Lysates were prepared and analyzed with immunoblotting. *CDC27-p*, phosphorylated CDC27. *B*, MAD2$^{(MCC)}$ is inactivated rapidly after RO3306-induced mitotic exit. Cells were treated as in *panel A*. The lysates were subjected to immunoprecipitation with antibodies against MAD2 and CDC20 before being analyzed with immunoblotting. *IP*, immunoprecipitates. *C*, MAD2$^{(APC/C)}$ remains intact after CDK1 inhibition. The experiment was performed as in *panel B* except that immunoprecipitation was performed with CDC27 antiserum. *D*, dissociation of MAD2$^{(MCC)}$ after CDK1 inhibition. Cells were blocked in prometaphase as described in supplemental Fig. S1. After treatment with RO3306 for 30 min, lysates were prepared and applied onto gel filtration chromatography. Fractions were collected, and the expression of the indicated proteins was analyzed with immunoblotting. *E*, proteasome activity is not required for the breakdown of MAD2$^{(MCC)}$. The experiment was performed as in *panel D* except that the cells were pretreated with MG132 for 1 h before RO3306 was added. *F*, depletion of CDC27 and APC2 impairs APC/C function. Cells were transfected with either control or siRNAs against CDC27 and APC2. The cells were preincubated with either buffer or MG132 for 1 h before being treated with RO3306 for 30 min. Lysates were prepared and analyzed by immunoblotting. *G*, inactivation of MAD2$^{(MCC)}$ but not MAD2$^{(APC/C)}$ requires APC/C activity. Cells were prepared exactly as in *panel F*. Lysates were subjected to immunoprecipitation with either MAD2 antiserum or APC4 antiserum. The indicated proteins were then detected by immunoblotting.

We further confirmed the above results by analyzing the MAD2 complexes with gel filtration chromatography. Fig. 5*D* shows that MAD2 already disappeared from the MCC fractions at 30 min after treating prometaphase cells with RO3306. The level of MAD2$^{(MCC)}$ was significantly reduced even in the presence of MG132 (Fig. 5*E*, *cf.* cells without RO3306 treatment in Fig. 2*C*). These data suggest that MAD2$^{(MCC)}$ was eliminated after CDK1 inactivation in a proteasome-independent manner.

To test more directly whether the inactivation of MAD2$^{(MCC)}$ was independent of protein degradation, the ubiquitin ligase activity of the APC/C was reduced by co-depletion of the CDC27 and APC2 (Fig. 5*F*). As expected, down-regulation of CDC27 and APC2 impaired APC/C activity, as indicated by the stabilization of prometaphase substrates including cyclin A2 and CDC20 (*lanes 1* and *5*). Degradation of cyclin B1 during RO3306-induced mitotic exit was also compromised (*lanes 2* and *6*).

Using this system, we found that the breakdown of MAD2$^{(MCC)}$ did not require APC/C activity because CDC20 disappeared from MAD2 immunoprecipitates even in CDC27- and APC2-depleted cells (Fig. 5*G*, *lanes 5* and *6*). By contrast, CDC20 and MAD2 remained bound to APC4 under the same conditions, indicating that breakdown of MAD2$^{(APC/C)}$ was dependent on APC/C activity. In agreement with the above results using MG132 (Fig. 5*G*, *lanes 3* and *4*), these data indicate that removal of MAD2$^{(APC/C)}$ but not MAD2$^{(MCC)}$ was dependent on APC/C-dependent proteolytic activity.

MAD2$^{(MCC)}$ Is Dismantled instead of Incorporated into APC/C during Mitotic Exit—We propose a model in which both MAD2$^{(MCC)}$ and MAD2$^{(APC/C)}$ are present when the spindle-assembly checkpoint is active. After the checkpoint is satisfied during metaphase, MAD2$^{(MCC)}$ becomes destabilized, but MAD2$^{(APC/C)}$ remains intact. MAD2$^{(APC/C)}$ is finally also eliminated when CDC20 is degraded after anaphase.

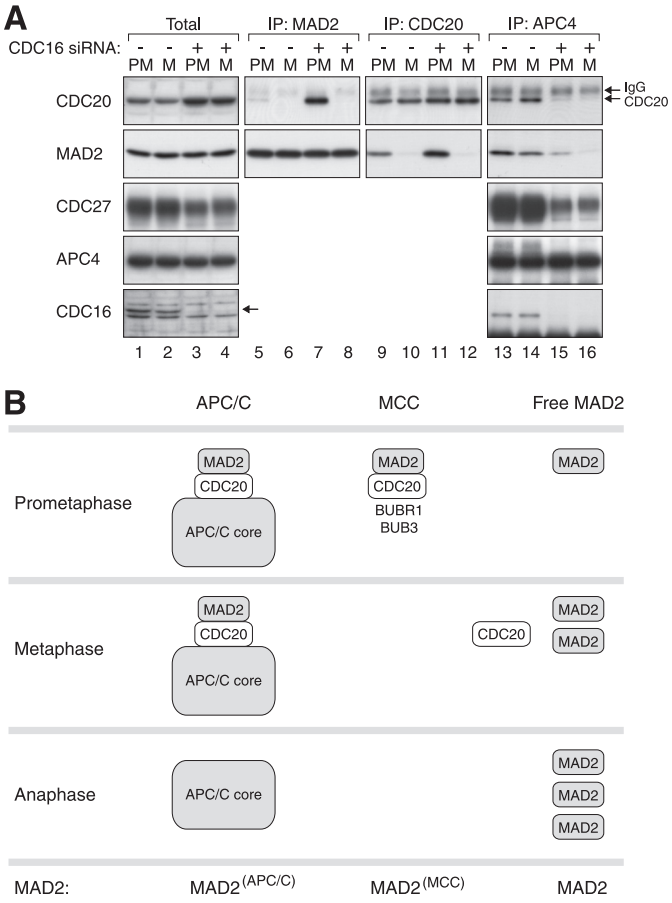

FIGURE 6. **MAD2$^{(MCC)}$ does not incorporate into APC/C after checkpoint satisfaction.** *A*, HeLa cells were transfected with either control or CDC16 siRNA. The transfection was performed at the same time as the addition of the first thymidine block. The subsequent synchronizations in prometaphase (*PM*) and metaphase (*M*) are identical to that described in supplemental Fig. S1. Lysates were prepared and subjected to immunoprecipitation with antibodies against MAD2, CDC20, or APC4. Total lysates and the immunoprecipitates (*IP*) were then analyzed with immunoblotting. *B*, a model of the regulation of MAD2-containing complexes during mitotic progression. Data from this study support an orderly inactivation of MAD2 during checkpoint recovery. The changes in the composition of different complexes are represented.

An alternative explanation of our data is nevertheless possible. It is conceivable that MAD2$^{(APC/C)}$ is actually broken down after checkpoint satisfaction but is then replenished by MAD2$^{(MCC)}$. The redistribution of MAD2 from MCC to APC/C may account for the selective disappearance of MAD2$^{(MCC)}$ during metaphase. To test this hypothesis, we took advantage of the fact that down-regulation of the CDC16 could disrupt the recruitment of CDC20 and MAD2 to APC/C (31). Fig. 6*A* shows that the recruitment of CDC20 and MAD2 to APC4 was significantly impaired after CDC16 was depleted with siRNA (*lanes 15* and *16*). It is interesting that the expression of CDC27 was also slightly reduced; we are currently unclear whether this was due to a specific effect of CDC16 depletion.

After CDC16 depletion, MAD2$^{(MCC)}$ could still be detected in prometaphase extracts (*lanes 7* and *11*). The abundance of MAD2$^{(MCC)}$ was in fact higher than in control cells, probably due to the stabilization of CDC20 (*lanes 3* and *4*). As in control cells, MAD2$^{(MCC)}$ was eliminated in metaphase (*lanes 8* and *12*), indicating that MAD2$^{(MCC)}$ was still removed in the absence of CDC16. These data suggest that the disappearance of MAD2$^{(MCC)}$ after checkpoint satisfaction was not due to a redistribution to APC/C.

DISCUSSION

One of the essential questions regarding mitotic exit is how the activated MAD2 is removed after the checkpoint is satisfied. In this report, we have focused our investigation on the dissociation of different MAD2 complexes. Our findings are consistent with the model that MAD2-containing complexes are removed in stages during mitotic progression (Fig. 6*B*).

Three populations of MAD2 were present when the spindle-assembly checkpoint was activated and could readily be resolved on a gel filtration column (Fig. 2*C*). After the checkpoint was satisfied, MAD2 disappeared from the MCC population with a concomitant increase in the relative level of free MAD2 (Fig. 2*D*). Meanwhile, the position of CDC20 was also shifted from the MCC to a smaller, presumably monomeric, form. Several other pieces of evidence support the selective dismantling of MAD2$^{(MCC)}$ during metaphase, including (*a*) the loss of MAD2$^{(MCC)}$ as revealed by co-immunoprecipitation studies (Fig. 1*A*); (*b*) the immediate reappearance of the complex when the checkpoint was reactivated with nocodazole (Fig. 1*D*); (*c*) the instability of MAD2$^{(MCC)}$ during the anaphase-like state induced by cyclin B1(NΔ) (Fig. 3); and (*d*) the selective elimination of MAD2$^{(MCC)}$ after CDK1 inactivation (Fig. 5*E*). In contrast to MAD2$^{(MCC)}$, MAD2$^{(APC/C)}$ remained intact during metaphase (Figs. 1*B* and 2). Interestingly, the existence of MAD2$^{(APC/C)}$ after checkpoint satisfaction implies that additional mechanisms may be involved in activating the MAD2-bound APC/C. However, a simpler explanation is that the APC/C activity was due to the MAD2-free APC/C; the MAD2$^{(APC/C)}$ was only dismantled later in anaphase, presumably when CDC20 was finally degraded (Figs. 4*D* and 5, *C* and *G*).

As checkpoint-satisfied extracts were prepared in the presence of MG132, our data suggest that MAD2$^{(MCC)}$ dissociation was independent of proteasome activity. Interestingly, these data are at odds with the recent results of Visconti *et al.* (32) showing that MAD2-CDC20 complexes (co-immunoprecipitation of MAD2 with an antibody against CDC20) persisted when cells were released from a nocodazole block into MG132. Our gel filtration chromatography and other data strongly supported that MAD2$^{(MCC)}$ was absent after the checkpoint was satisfied (Fig. 2*D*). One possible explanation that could reconcile this discrepancy is that the anti-CDC20 immunoprecipitation procedure used by Visconti *et al.* (32) could isolate both MAD2$^{(APC/C)}$ and MAD2$^{(MCC)}$.

Conceptually, the free MCC and APC/C-MCC should be disassembled for APC/C reactivation. In a HeLa cell extracts model, ubiquitination by APC/C can drive the dissociation of checkpoint components from APC/C (33), which is consistent with our data. More recently, it was found that the cleavage of ATP at the β-γ position, which is not required for ubiquitination, is essential for the MCC dissociation in HeLa cell extracts (34). Our data also supported the differential regulation in MCC and APC/C-MCC dissociation. In addition, our data fur-

ther suggested a temporal difference in disassembly of checkpoint components of the MCC and APC/C.

Although the present work provided insights into a possible differential regulation of different MAD2-containing complexes during checkpoint inactivation, it raised several new questions. Foremost, what are the mechanisms involved in selectively dismantling $MAD2^{(MCC)}$? Spatial differences with $MAD2^{(APC/C)}$ could be a possible mechanism. Given that both inactive and active APC/C in prometaphase and metaphase, respectively, appear to associate with MAD2, what is the molecular basis of the control of APC/C? A possible solution is that the relief of the inhibition of MAD2 on APC/C may not require dissociation. For example, the MAD2-binding protein $p31^{comet}$ is proposed to regulate the silencing of the spindle-assembly checkpoint by neutralizing the effect of MAD2 on CDC20, and $p31^{comet}$ can stimulate the activity of APC/C without disrupting the MAD2-CDC20 interaction (35). An alternative solution is that MAD2-independent mechanisms may be involved in turning off of APC/C activity, such as that proposed for MCF2 (36).

Acknowledgments—Many thanks are due to members of the Poon laboratory for constructive criticism on the manuscript. We thank Mingjie Zhang for help with gel filtration experiments.

REFERENCES

1. Pesin, J. A., and Orr-Weaver, T. L. (2008) *Annu. Rev. Cell Dev. Biol.* **24,** 475–499
2. Musacchio, A., and Salmon, E. D. (2007) *Nat. Rev. Mol. Cell Biol.* **8,** 379–393
3. Vigneron, S., Prieto, S., Bernis, C., Labbé, J. C., Castro, A., and Lorca, T. (2004) *Mol. Biol. Cell* **15,** 4584–4596
4. Nilsson, J., Yekezare, M., Minshull, J., and Pines, J. (2008) *Nat. Cell Biol.* **10,** 1411–1420
5. Fang, G. (2002) *Mol. Biol. Cell* **13,** 755–766
6. Tang, Z., Bharadwaj, R., Li, B., and Yu, H. (2001) *Dev. Cell* **1,** 227–237
7. Luo, X., Tang, Z., Rizo, J., and Yu, H. (2002) *Mol. Cell* **9,** 59–71
8. De Antoni, A., Pearson, C. G., Cimini, D., Canman, J. C., Sala, V., Nezi, L., Mapelli, M., Sironi, L., Faretta, M., Salmon, E. D., and Musacchio, A. (2005) *Curr. Biol.* **15,** 214–225
9. Pinsky, B. A., Nelson, C. R., and Biggins, S. (2009) *Curr. Biol.* **19,** 1182–1187
10. Vanoosthuyse, V., and Hardwick, K. G. (2009) *Curr. Biol.* **19,** 1176–1181
11. Ma, H. T., Tsang, Y. H., Marxer, M., and Poon, R. Y. (2009) *Mol. Cell. Biol.* **29,** 6500–6514
12. Chan, Y. W., Ma, H. T., Wong, W., Ho, C. C., On, K. F., and Poon, R. Y. (2008) *Cell Cycle* **7,** 1449–1461
13. Arooz, T., Yam, C. H., Siu, W. Y., Lau, A., Li, K. K., and Poon, R. Y. (2000) *Biochemistry* **39,** 9494–9501
14. Poon, R. Y., Toyoshima, H., and Hunter, T. (1995) *Mol. Biol. Cell* **6,** 1197–1213
15. Ausubel, F., Brent, R., Kingston, R., Moore, D., Seidman, J., Smith, J., and Struhl, K. (eds) (1991) *Current Protocols in Molecular Biology*, pp. 9.1.1–9.1.11, John Wiley & Sons, New York
16. Yam, C. H., Siu, W. Y., Kaganovich, D., Ruderman, J. V., and Poon, R. Y. (2001) *Proc. Natl. Acad. Sci. U.S.A.* **98,** 497–501
17. Li, K. K., Ng, I. O., Fan, S. T., Albrecht, J. H., Yamashita, K., and Poon, R. Y. (2002) *Liver* **22,** 259–268
18. Wassmann, K., and Benezra, R. (1998) *Proc. Natl. Acad. Sci. U.S.A.* **95,** 11193–11198
19. Li, Y., Gorbea, C., Mahaffey, D., Rechsteiner, M., and Benezra, R. (1997) *Proc. Natl. Acad. Sci. U.S.A.* **94,** 12431–12436
20. Bellanger, S., de Gramont, A., and Sobczak-Thépot, J. (2007) *Oncogene* **26,** 7175–7184
21. Sudakin, V., Chan, G. K., and Yen, T. J. (2001) *J. Cell Biol.* **154,** 925–936
22. Dantuma, N. P., Groothuis, T. A., Salomons, F. A., and Neefjes, J. (2006) *J. Cell Biol.* **173,** 19–26
23. Chang, D. C., Xu, N., and Luo, K. Q. (2003) *J. Biol. Chem.* **278,** 37865–37873
24. Pan, J., and Chen, R. H. (2004) *Genes Dev.* **18,** 1439–1451
25. Reis, A., Levasseur, M., Chang, H. Y., Elliott, D. J., and Jones, K. T. (2006) *EMBO Rep.* **7,** 1040–1045
26. Kramer, E. R., Scheuringer, N., Podtelejnikov, A. V., Mann, M., and Peters, J. M. (2000) *Mol. Biol. Cell* **11,** 1555–1569
27. Chow, J. P., Poon, R. Y., and Ma, H. T. (2011) *Mol. Cell. Biol.*, in press
28. D'Angiolella, V., Mari, C., Nocera, D., Rametti, L., and Grieco, D. (2003) *Genes Dev.* **17,** 2520–2525
29. Vassilev, L. T., Tovar, C., Chen, S., Knezevic, D., Zhao, X., Sun, H., Heimbrook, D. C., and Chen, L. (2006) *Proc. Natl. Acad. Sci. U.S.A.* **103,** 10660–10665
30. Skoufias, D. A., Indorato, R. L., Lacroix, F., Panopoulos, A., and Margolis, R. L. (2007) *J. Cell Biol.* **179,** 671–685
31. Rudner, A. D., and Murray, A. W. (2000) *J. Cell Biol.* **149,** 1377–1390
32. Visconti, R., Palazzo, L., and Grieco, D. (2010) *Cell Cycle* **9,** 564–569
33. Reddy, S. K., Rape, M., Margansky, W. A., and Kirschner, M. W. (2007) *Nature* **446,** 921–925
34. Teichner, A., Eytan, E., Sitry-Shevah, D., Miniowitz-Shemtov, S., Dumin, E., Gromis, J., and Hershko, A. (2011) *Proc. Natl. Acad. Sci. U.S.A.* **108,** 3187–3192
35. Xia, G., Luo, X., Habu, T., Rizo, J., Matsumoto, T., and Yu, H. (2004) *EMBO J.* **23,** 3133–3143
36. Eytan, E., Braunstein, I., Ganoth, D., Teichner, A., Hittle, J. C., Yen, T. J., and Hershko, A. (2008) *Proc. Natl. Acad. Sci. U.S.A.* **105,** 9181–9185